In-situ generated graphene from wheat flour for enhancing mechanical and electrical properties of copper matrix composites

Tao Yang[1], Wenge Chen[1 *], Hui Zhang[1], Longhai Ma[1], Yong-Qing Fu[2 *]

[1] School of Materials Science and Engineering, Xi'an University of Technology, Xi'an, Shaanxi, 710048, P.R. China.

[2] Faculty of Engineering and Environment, Northumbria University, Newcastle upon Tyne, NE1 8ST, UK.

Abstract: Graphene, with its excellent mechanical properties and electrical conductivity, has been considered as an effective reinforcement phase for copper matrix composites. However, due to its easy agglomeration and poor wetting properties in the copper matrix, it is difficult to simulataneously enhance strength, ductility and conductivity of graphene based copper composites using a low cost and efficient method. In this paper, we proposed a new methodology to use wheat flour as a solid carbon source to *in-situ* generate graphene-coated copper (Gr@Cu) composite powders. These powders were then used as strengthening phases to fabricate Gr@Cu copper composites through wet mixing and spark plasma sintering (SPS) processes. Results showed that not only high-quality graphene layer was obtained and serious agglomeration of graphene was avoided, but also a strong interfacial bonding between

[*] Corresponding authors: Prof. Wenge Chen; Prof.Richard Y.Q.Fu.

E-mail: wgchen001@263.net (W.G. Chen), richard.fu@northumbria.ac.uk (Richard Y.Q. Fu)

graphene and copper matrix was achieved. The fabricated composites showed excellent properties, e.g., a maximum density of 99%, enhanced micro-hardness (15%-22% higher than that of pure copper), and excellent strength/ ductility. The maximum tensile strength and yield strength were obtained in the 0.70 wt.%Gr@Cu/Cu composites (e.g., 252 MPa and 132 MPa, respectively). These values are ~23% and ~110% higher than those of pure copper, and the elongation rate was maintained at ~30%. In addition, the composites showed excellent conductivity.

Keywords: Copper Matrix Composites, Graphene, Mechanical Properties, Conductivity

1. Introduction

Copper has excellent electrical and thermal conductivities and has been extensively used in the fields such as power transportation (wires or cables) and electronics (electric connectors) [1]. However, its low strength and poor hardness often restrict its wide-range applications. At present, its strengthening methods can be divided into two categories. The first one is alloying, in which metal elements are added into copper to form a solid solution thus improving the mechanical properties of copper, e.g., Cu-Cr-Zr, Cu-Fe-P, and Cu-Ni-X [2-4]. However, it is well known that mechanical properties and functional properties of these composites are often difficult to enhance simultaneously. For example, a large increase in mechanical properties of copper alloys often deteriorates their conductivity. Another strengthening method is adding ceramic particles such as oxides (Al_2O_3, SiO_2),

carbides (TiC, WC, SiC), nitrides (TiN), borides (TiB_2, ZrB_2), or other fiber reinforcements (e.g., carbon fiber, tungsten fiber, boron fiber, etc.) [5, 6]. However, for this strengthening method, there are often problems such as deteriorated physical properties (e.g., electrical conductivity and thermal conductivity) [5, 6].

Graphene (Gr) has recently become one of the most attractive carbon reinforcements in copper matrix composites due to its unique structure and excellent performance. However, graphene is easily agglomerated in the copper matrix and the wetting angle between graphene and copper is very high, e.g., ~140°. This non-wetting feature [7] makes it a great challenge to achieve good physical, mechanical and functional properties of graphene enhanced copper composites. Therefore, a lot of studies on graphene reinforced copper (Gr/Cu) matrix composites have been focused on preventing agglomeration of graphene and achieving strong interfacial bonding between graphene and copper matrix [8-14].

At present, a variety of preparation methods of Gr/Cu composites have been developed, including powder metallurgy, molecular-level mixing technology, and *in-situ* generation technology [8-10]. For example, Yue et al. [15] used a high-energy ball milling method to disperse graphene nanoparticles (GNPs) uniformly inside a copper matrix. They reported that the large shear force during high-energy ball milling caused damage to the internal structures of GNPs, which had a negative impact on the properties of the copper matrix. Hwang et al. [16] used a molecular-level mixing technology to prepare reduced graphene oxide/copper (rGO/Cu) composites. They reported that a high degree of defects in the rGO

significantly reduced the inherent conductivity of the copper matrix, even though the mechanical properties have been improved.

To achieve a uniform dispersion of graphene inside the copper matrix composite, some researchers used chemical vapor deposition (CVD) to coat a layer of graphene on the surfaces of copper particles before the thermal consolidation process [11-14, 17]. However, using such graphene precursors in the CVD process has certain drawbacks. For examples, this will cause problems for consolidation of copper powders due to high decomposition temperatures of gas precursors during *in-situ* graphene generation process, and the liquid precursor also causes uneven distribution of the carbon sources. Therefore, other researchers tried to use solid precursors. For example, Dong et al. [11] used polymethyl methacrylate (PMMA) as a carbon source to *in situ* generate graphene on the surface of copper powder, and reported that the syntheized composites achieved a high tensile strength of 260 MPa and a conductivity of 75.5% IACS (International Annealing Copper Standard). Sun et al. [12] used glucose to *in-situ* generate high-quality graphene on the surface of copper powder and then studied effect of sintering temperature on the properties of the composite materials used a spark plasma sintering (SPS) method. They reported that the graphene-coated copper (Gr@Cu) composite powders pre-prepared by the CVD method were uniformly dispersed inside the copper matrix. Yang et al. [13] applied oleic acid as the graphene precursor, and reported that tensile strength of composites prepared using this method was 432 MPa, but elongation ratio was as low as 0.45%. Wang et al. [14] used small aromatic hydrocarbons to *in-situ* generate graphene on

copper substrates, however, they found that the tensile strength of the fabricated composites obtained using an SPS process was even lower than that of pure copper.

Clearly it is a great challenge to use solid carbon sources for achieving comprehensive properties (including high strength, high conductivity, and good ductility) of the graphene reinforced copper matrix composites. From the perspectives of low production cost and efficiency, *in-situ* production technology would have its great advantages for fabricating graphene reinforced copper matrix composites. However, many solid carbon sources are not cheap and difficult to obtain. Therefore, it is of great interests to apply cheap and widely available solid carbon sources as precursors for *in-situ* generation of graphene on surfaces of Cu particles and to explore the relationships between interfacial microstructure and properties of the obtained composites.

In this paper, wheat flour, which is cheap and widely available, is chosen to *in-situ* form high-quality graphene on the surfaces of copper powders (e.g., Gr@Cu). The high carbon-oxygen ratio (6:5) in wheat flour ensures that carbon atoms will not be easily consumed by oxygen atoms during the synthesis process, thus providing enough source for generation of graphene. Using wet mixing and SPS technologies, Gr@Cu reinforced copper matrix composites (Gr@Cu/Cu) with different contents of Gr@Cu composite powders have been obtained. The interfacial bonding and distributions of graphene in the copper matrix of Gr@Cu composite powder have been thoroughly investigated and then linked with mechanical and electrical properties of the sintered composites.

Fig. 1 schematically illustrates the strengthening mechanism of the copper matrix synthesized using the Gr@Cu composite powders. As shown in Fig. 1(a), the Gr@Cu composite powder has a good bonding with the copper matrix. When there is an external stress applied, deformation will be firstly happened in the copper matrix (Fig. 1(b)). The copper matrix undergoes a plastic fracture, but then is partially broken as shown in Fig. 1(c), while the Gr@Cu particles have a good bridging effect for enhancing the toughness of the composites. With further increase of the stress, the load is transferred to the Gr@Cu reinforced particles through their interfaces. The Gr@Cu particles will undergo fracture, which provides the high strength of the composite. The high electrical conductivity can also be effectively provided by the Cu substrates and the uniformly distributed Gr@Cu particles.

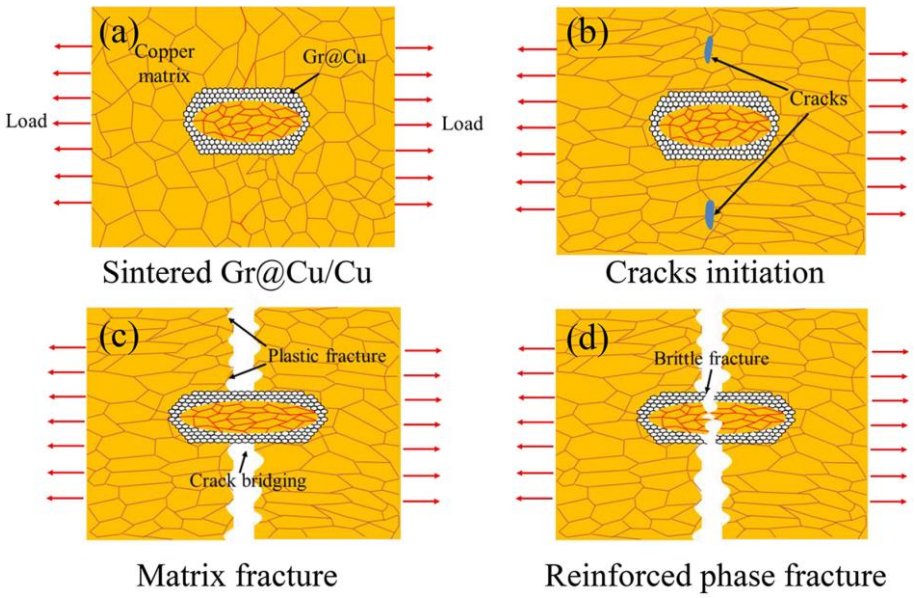

Fig. 1 Schematic illustrations of strengthening mechanism of Gr@Cu composite powder strengthening the copper matrix. (a) Good interface bonding between Gr@Cu and copper matrix; (b) Crack generation in the copper matrix under the externally applied load; (c) The copper matrix first undergoes plastic deformation and then

fracture, while the bridging effects of the Gr@Cu can provide a high ductility of the composite; (d) The load is effectively transferred to the Gr@Cu reinforced phase through the interface, and the Gr@Cu finally undergoes a brittle fracture under a large stress, ensuring the high strength of the composite

2. Materials and experiments

2.1 Materials

Copper powders (purity 99.9% with diameters of 35-38 μm) were purchased from Beijing Xingrongyuan Technology Co., Ltd., China. Wheat flour (universal wheat flour) was purchased from China Resources Vanjia Convenient Supermarket. The rest of the reagents were of analytical grades and used directly without further purification.

2.2 Preparation of Gr@Cu/Cu composite powder

To prepare Gr@Cu composite powder, wheat flour (0.5 g) and pure copper powder (10 g) were ball-milled with a ball-to-material ratio of 10:1 at a speed of 423 rpm for 5 h, and wheat flour-coated copper powder of 0.5 g was obtained. Then the powder was loaded into a vacuum tube furnace, whose temperature was increased to 800°C with a heating rate of 10 min/°C. The temperature was maintained for 10 min, under a continuous gas flow (40 sccm H_2 and 100 sccm Ar) throughout the process. To estimate the content of graphene in the composite powder, 3 g of Gr@Cu composite powder was etched using 20 wt.% nitric acid for 48 hours to completely remove the copper matrix. Corrosion products of 0.0702 was obtained, which has ~2.34 wt.% of graphene.

Three different types of Gr@Cu composite powders (e.g., 0.35 wt.%, 0.70 wt.%, and 1.05 wt.% of graphene in the composite) and pure copper powders were selected for wet mixing. The detailed process is illustrated in Fig. 2(a). The Gr@Cu composite powder and pure copper powder were mixed with 200 mL of absolute ethanol at room temperature inside a beaker. They were ultrasonically agitated with a power of 90 W for 1 h. Then the solution of composite powder was put into a magnetic stirrer (65°C, 800 rpm). During the mechanical stirring process, the absolute ethanol was volatilized, and a uniformly mixed Gr@Cu/Cu composite powder was obtained. These three different composite powders were named as 0.35 wt.%Gr@Cu/Cu, 0.70 wt.%Gr@Cu/Cu, and 1.05 wt.%Gr@Cu/Cu, respectively.

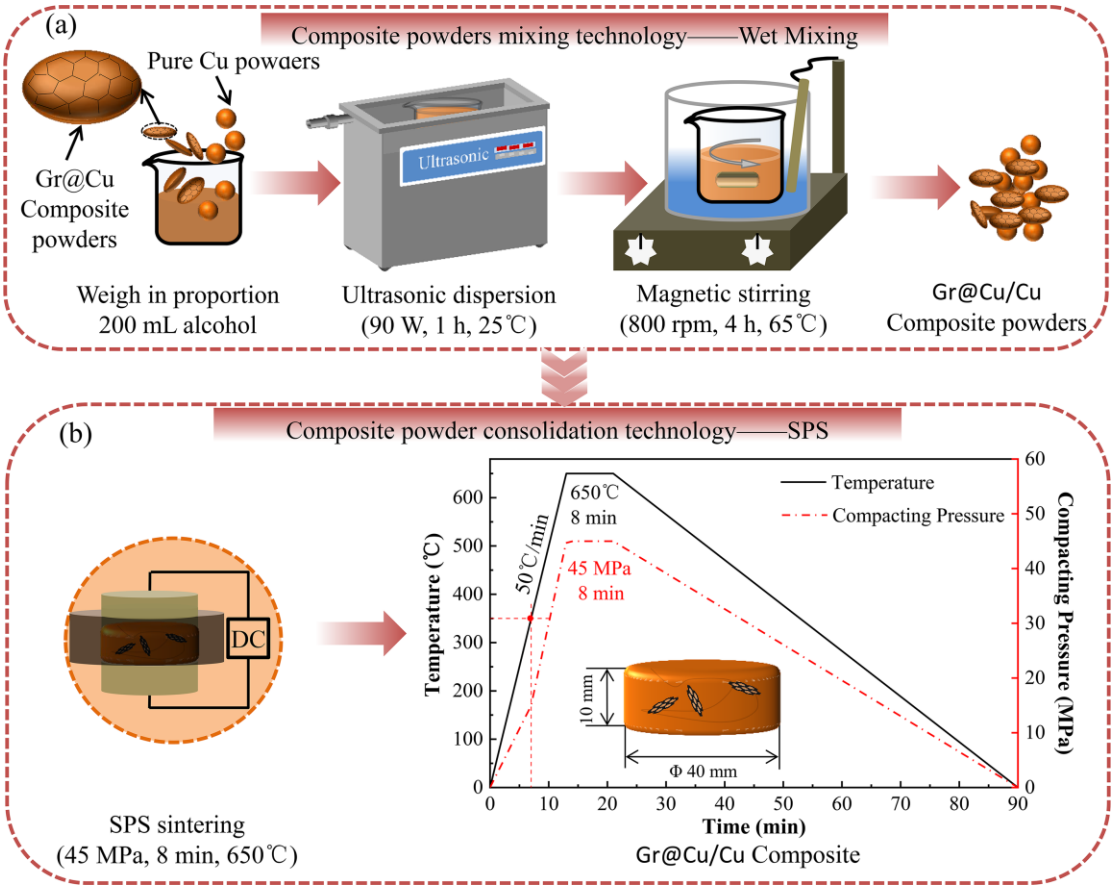

Fig. 2 Schematic illustrations of the preparation process of Gr@Cu/Cu composite powders and composites. (a) Gr@Cu/Cu composite powders, (b) Gr@Cu/Cu composites

2.3 Preparation of Gr@Cu/Cu composite

The mixed Gr@Cu/Cu composite powder was transferred into an SPS furnace, and sintered at a temperature of 650 ℃, a pressing pressure of 45 MPa, and a sintering time of 8 min. Gr@Cu/Cu composites with a dimension of ϕ40 mm×10mm were obtained. The detail of SPS process is shown in Fig. 2(b). The heating rate was 50 ℃/min, and the sintering pressure was gradually increased up to 15 MPa from 25~350 ℃. The sintering pressure was rapidly increased to 45 MPa from 350~650 ℃. As the temperature reached 650 ℃, the pressure was maintained for 8 minutes. The obtained composites were named as 0.35 wt.%Gr@Cu/Cu, 0.70 wt.%Gr@Cu/Cu, and 1.05 wt.%Gr@Cu/Cu composites, respectively. In addition, under the same sintering conditions, pure copper was also obtained as a control sample.

2.4 Characterization

X-ray diffractometer (XRD, XRD-7000S, Japan) was used to analyze the crystalline phases of graphene/copper composites and pure copper blocks, with CuKα radiation (wavelength of 1.5418Å) and a scanning speed of 8 °/min. A scanning electron microscope (SEM, Quanta-450-FEG, USA) was used to observe the morphology of the composite and the distribution of graphene. Energy dispersive X-ray spectroscopy (EDS) was used to evaluate if the graphene was uniformly distributed inside the copper matrix. The microstructure of graphene was

characterized using a high-resolution transmission electron microscope (HRTEM, JEM-3010, Japan), and the lattice fringe and interface characteristics of graphene and copper matrix were characterized. A digital conductivity meter (D60K, China) was used to measure the conductivity of the composite materials (%IACS). Micro-hardness of the composite material was characterized using a Vickers hardness tester (HV-120, China), with an indentation load of 5 kg and a loading time of 10 s. A computer-controlled universal testing machine (HT-2402, China) was used to characterize tensile strength, yield strength, and elongation of the composite. The sintered composite was subjected to wire cutting and polishing to obtain tensile specimens. The sample size was 20 mm in gauge length, 4 mm in width, and 1.5 mm in thickness. The tensile test was carried out at a loading speed of 1 mm/min at room temperature. Three tensile specimens were prepared for each composite material. The density (ρ) of the composite material was measured using the Archimedes method. The theoretical density (ρ_0) of the composite material was obtained using formula (1), , and the density (φ) of the bulk material was obtained using formula (2).

$$\rho_0 = \frac{m_{Cu}+m_{Gr}}{\frac{m_{Cu}}{\rho_{Cu}}+\frac{m_{Gr}}{m_{Gr}}} \quad (1)$$

$$\varphi = \frac{\rho}{\rho_0} \times 100\% \quad (2)$$

where m_{Cu} and m_{Gr} are the masses of the copper matrix and graphene in the composite material, and ρ_{Cu} and ρ_{Gr} are 8.96 g/cm^3 and 2.2 g/cm^3, respectively.

3. Results and discussion

3.1 Structure and phase analysis of Gr@Cu composite powder

Figs. 3(a) and 3(b) show images of pure copper and Gr@Cu composite powders, respectively. The color of the copper powder (yellow-brown) is clearly changed into gray-black after coated with a layer of graphene. To verify that the etching method can obtain the graphene in the Gr@Cu composite powder, the composite sample was etched with 20 wt.% nitric acid for 24 hrs and 48 hrs, respectively (Fig. 3 (c)). The etched products were analyzed using XRD. It can be seen that the copper matrix cannot be completely removed after etching for 24 h, whereas the copper matrix has been completely etched away after 48 h. This clearly indicates that the graphene has been successfully obtained on the Cu surface by etching for 48 h. The corrosion product (24 h) has a broad XRD peak at 26°, which corresponds to the peak of graphene. A weak graphene oxide (GO) peak appears at around 12°, and the GO peak becomes sharper with the increase of the etching time. The reason is that part of the graphene was oxidized during the acid etching process. Surprisingly, after etched for 48 h, the corrosion product has a weak diffraction peak at 43.6°, which might be also linked to the graphene peak [18].

Fig. 4 shows TEM images of the composites. From Fig. 4(a), it can be seen that the copper particles are surrounded by a layer of transparent and gauze-like substance. In Fig. 4(b), two kinds of fringes with completely different lattice fringe spacings and orientations can be clearly observed. The lattice fringe spacing of the outer layer is ~0.355 nm, which is similar to the Gr (002) crystal plane (Fig. 4(c)). From Fig. 4(c), it can be observed that the graphene layer is approximately ~2 nm thick, which is about

4~6 layers. The interface between graphene and copper substrate is smooth and well bonded.

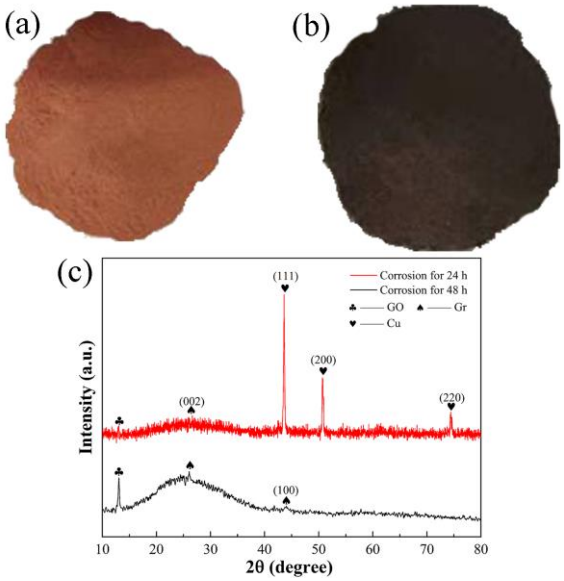

Fig. 3 Images of (a) Pure copper, (b) Gr@Cu composite powder (c) XRD patterns of corrosion products

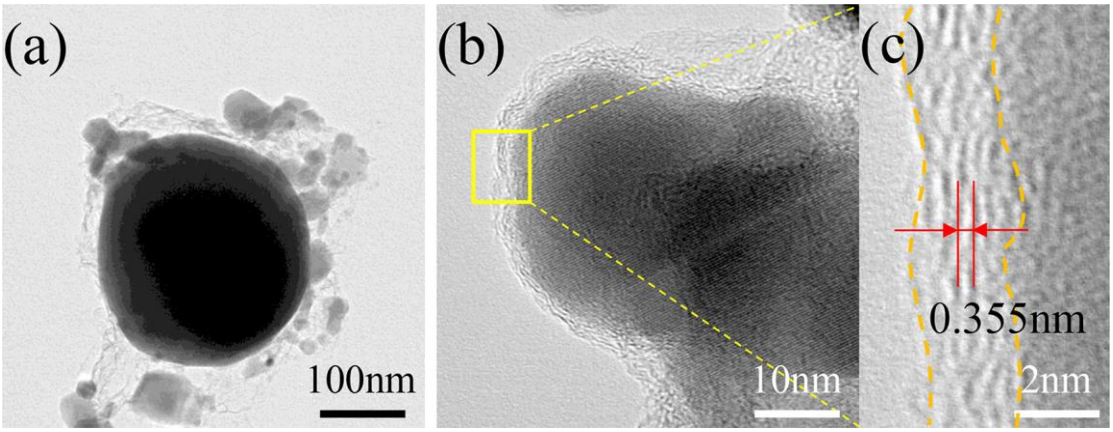

Fig. 4 TEM and HRTEM images of Gr@Cu composite powder. (a) TEM, (b) HRTEM, (c) the magnified region of of the yellow box in (b)

3.2 Microstructure of Gr@Cu /Cu composite

As shown in Fig. 5, all the three types of composite materials have diffraction peaks around 43°, 50°, and 74°, corresponding to the (111), (200), and (220) crystal

planes of pure copper, respectively. There is no graphene diffraction peak in the XRD pattern of the composite, probably because the content of graphene is lower than the lower limit of XRD detection. This result is consistent with those reported by Sun et al. [12], which was obtained from a Gr/Cu composite prepared by SPS. After the graphene is added, the diffraction peaks of the composite materials are shifted to the right-hand side, because the atomic radius of the graphene is smaller than that of the copper atom. This shift might be also caused by the residual stresses in the composite.

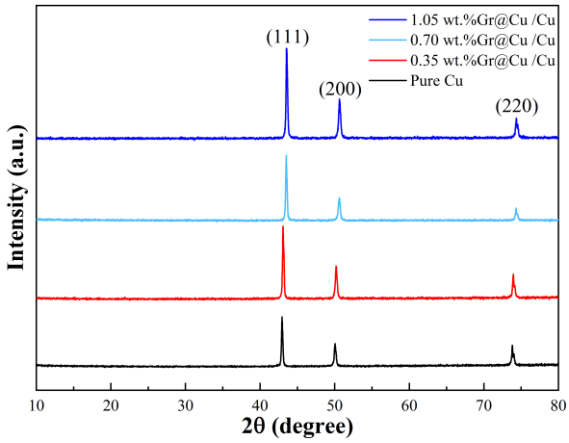

Fig. 5 XRD patterns of pure copper and Gr@Cu/Cu composites

Fig. 6 shows SEM images of the composites after sintering. The surface of pure copper is smooth with a few holes and defects (Fig. 6(a)). The morphology of the Gr@Cu/Cu composites shows that the black areas are increased with the increase of the graphene content. EDS analysis of these black matter shows that they contain C and Cu elements. The Gr reinforcement phases of 0.35 wt.% Gr@Cu/Cu and 0.70 wt.% Gr@Cu/Cu composites are quite uniform, whereas the 1.05 wt.% Gr@Cu/Cu composite shows apparent agglomeration. Hole defects (as shown with black arrows in Figs. 6 (b), (c), and (d)) can be seen, indicating that the density of the composite has not reached 100%.

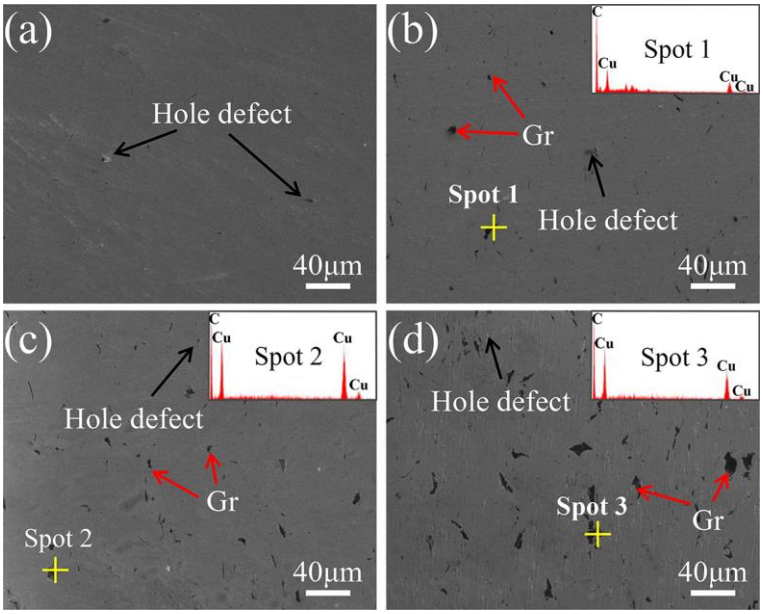

Fig. 6 SEM images and EDS results of the microstructure of pure copper and Gr@Cu /Cu composites. (a) Pure copper, (b~d) SEM images of 0.35 wt.%Gr@Cu/Cu, 0.70 wt.%Gr@Cu/Cu, and 1.05 wt.%Gr@Cu/Cu. The illustrations are the EDS images of Spot 1, Spot 2, and Spot 3

3.3 Properties of sintered Gr@Cu/Cu composite

Table 1 summarizes the obtained density values of the sintered pure copper and composite materials. Due to the low density of graphene, the measured densities of the composites show a decreasing trend with the increased content of graphene, which is consistent with the results reported by Rajkumar et al. [19]. The relative density of composite materials is above 99% but not reaching 100%, as shown in Fig. 6. However, compared with the density of Gr/Cu composites obtained using a vacuum hot pressing sintering method (92.6%) [20] and a microwave sintering method (92%) [21], the data obtained from the SPS sintering process in this study are much higher.

Table 1 Density value of pure copper and composites

Sample	Measured density (g/cm^3)	Theoretical density (g/cm^3)	Relative density (%)
Pure Cu	8.87 (±0.01)	8.96	99.0
0.35 wt.%Gr@Cu/Cu	8.79 (±0.03)	8.86	99.2
0.70 wt.%Gr@Cu/Cu	8.71 (±0.01)	8.77	99.3
1.05 wt.%Gr@Cu/Cu	8.63 (±0.01)	8.68	99.4

The reason for such a high density of the composite in this study is because the slowly increased sintering pressure applied in the early stage of sintering (~350°C) helps to effectively reduce the gas trapped among the powders. A rapidly increased sintering pressure was applied during the increase of temperature in the chamber, so that the gas adsorbed on the surface of the powder was easily escaped during the heating process, thus achieving a high density of composites. The wet powder mixing process also made the graphene dispersed well in the copper matrix without serious agglomeration, which contributes to the high sintering density [19].

Fig. 7 shows micro-hardness and conductivity values of pure copper and composites. The micro-hardness values of the composites are 15%-22% higher than that of pure copper, which indicates that the pre-prepared Gr@Cu composite powder is effective in reinforcing the copper matrix. Among them, the 1.05 wt.%Gr@Cu/Cu composite shows the highest micro-hardness value of 95 HV, which is about 22% higher than that of pure copper (i.e., 78 HV). Compared with that of pure copper, the micro-hardness values of 0.35 wt.%Gr@Cu/Cu and 0.70 wt.%Gr@Cu/Cu composites are increased by 15% and 18%, respectively. It can be concluded that the

micro-hardness value of the composite increases slightly with the increase of the amount of graphene added. However, Yue et al. [15] reported that the microhardness of the graphene enhanced copper composite was decreased when the content of graphene was above 1 wt%. They explained that high content of graphene (1.0 wt.%, 2.0 wt.%) caused serious agglomeration and thus the micro-hardness of the composite was decreased. However, the micro-hardness of the composite in this study did not show any decrease. When the graphene content is not added above a threshold value, graphene is evenly distributed in the copper matrix, without apparent agglomeration. This ensures that the composite has a good dispersion strengthening effect [15, 22].

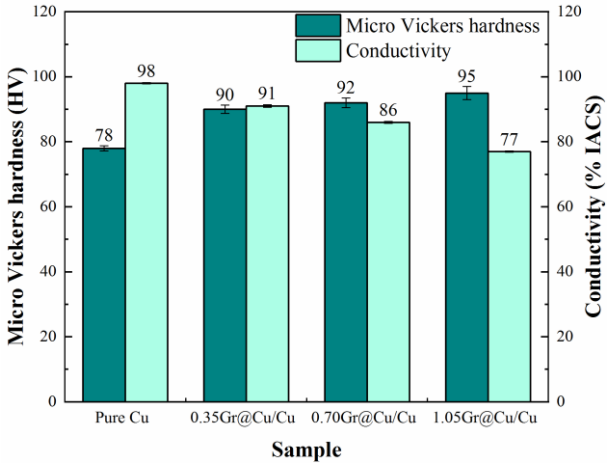

Fig. 7 Micro-hardness and conductivity values of pure copper and composites

For pure copper and composites, the changing trend of the conductivity values is exactly the opposite to that of the micro-hardness value. With the increase of graphene content, the conductivity of composites shows a downward trend, which is mainly due to: (1) increased interfaces, degree of electron scattering and interface resistances [23]; and (2) increased agglomeration of graphene (Fig. 6(d)). Both of these two factors affect the electrical conductivity of the composite. The sintered pure

copper shows the best conductivity value (98% IACS), whereas 0.35 wt.% and 0.70 wt.% Gr@Cu/Cu composites have conductivity values of 91% IACS and 86% IACS, respectively. The conductivity value of 1.05 wt.%Gr@Cu/Cu composite is decreased to 77% IACS, which is unsuitable for many industry applications (>80% IACS). It is worth mentioning that although the conductivity values of the composites are lower than that of pure copper, they are still significantly higher than those of copper matrix composites synthesized using the other methods or reinforcing phases (see Table 2). The key reason for this good performance is that the Gr@Cu reinforcement used in this paper has excellent electrical conductivity, as the graphene has a carrier mobility of 2.0×10^5 $cm^2/(V\cdot s)$. In addition, for the composites with graphene concentrations of 0.35 wt.% and 0.70 wt.%, the threshold value of the graphene has not reached, and there is no apparent agglomeration of the graphene, thereby avoiding the potential electron scattering effect and ensuring a good conductivity.

Table 2 Comparisons of conductivity values and mechanical properties obtained from this work and those copper matrix composites reported in literature

Sample	Preparation method	Conductivity （%IACS）	Yield Strength (MPa)	Ultimate tensile strength (MPa)	Elongation (%)	Ref.
0.35 wt.%Gr@Cu/Cu	SPS	90	107	232	40	This work
0.70 wt.%Gr@Cu/Cu	SPS	86	132	252	30	This work
0.30 wt.%rGO/Cu	SPS	73.4	156	163	8	[24]
15 vol.%CNTs/Cu	SPS	75	-	342	1.2	[25]
5 vol.%Al_2O_3/Cu	Hot extrusion	44.2	620	775	11	[26]

Fig. 8(a) shows engineering stress-strain curves of the sintered pure copper and composites. There are three stages observed, including elastic deformation, uniform plastic deformation, and fracture [27]. After adding the graphene into the copper matrix, the strength is significantly higher than that of pure copper, whereas the plasticity is reduced, as shown in Fig. 8(c). Compared with the sintered pure copper, it can be seen that the ultimate tensile strength of 0.35 wt.%Gr@Cu/Cu composite is increased by about 14% to 232 MPa, and the yield strength is significantly increased by about 70% to 107 MPa. At the same time, compared with the elongation of pure copper (47%), although there is a slight decrease of the elongation of 0.35 wt.%Gr@Cu/Cu composite, it still maintains a high level of 40%. The maximum values of ultimate tensile strength and yield strength in this study have been found in the 0.70 wt.%Gr@Cu/Cu composite material, which are 252 MPa and 132 MPa, respectively, These values are increased by about 23% and 110%, respectively, compared with those of the sintered pure copper. In addition, the elongation has been maintained at about 30%, showing that these composites have both high strength and high plasticity. However, with further increase of the amount of Gr@Cu composite powder, the strength of 1.05 wt.% Gr@Cu/Cu composite decreases. Compared with the results of graphene reinforced copper composites synthesized using the other methods, the composite in this study does not show much higher strength. However, the composite obtained in this paper has its advantages of achieving good plasticity and ductility (see Table 2).

A previous study [11] showed that the higher the work hardening rate, the stronger the resistance to deformation, the faster the dislocation storage speed, and the more effective for the strengthening effect. Fig. 8(b) shows the true stress-true strain curve and true strain-hardening rate curve of sintered copper and composites. From Fig. 8(b), the hardening rate of the composites was decreased much faster than that of pure copper in the initial stage, indicating that the composite can quickly obtain a high yield strength. The hardening rate of 0.70 wt.%Gr@Cu/Cu composite is significantly larger than those of the other samples.

To evaluate the synergistically improved electrical and mechanical properties, we applied a comprehensive index of plasticity (e.g., using the empirical formula of $K_{IC}=0.32\sqrt{\pi E\sigma_b\delta_k\rho_c}$, proposed by Zheng [28] et al.) as the ordinate and conductivity as the abscissa. Compared to those of copper matrix composites enhanced with rGO, the primeval graphite, metal nanoparticles modified rGO, GNPs and *in-situ* Gr [22, 24, 29-35] shown in Fig. 8(d), the copper matrix composite material obtained in this study has excellent comprehensive properties (e.g., mechanical properties, and electrical conductivity).

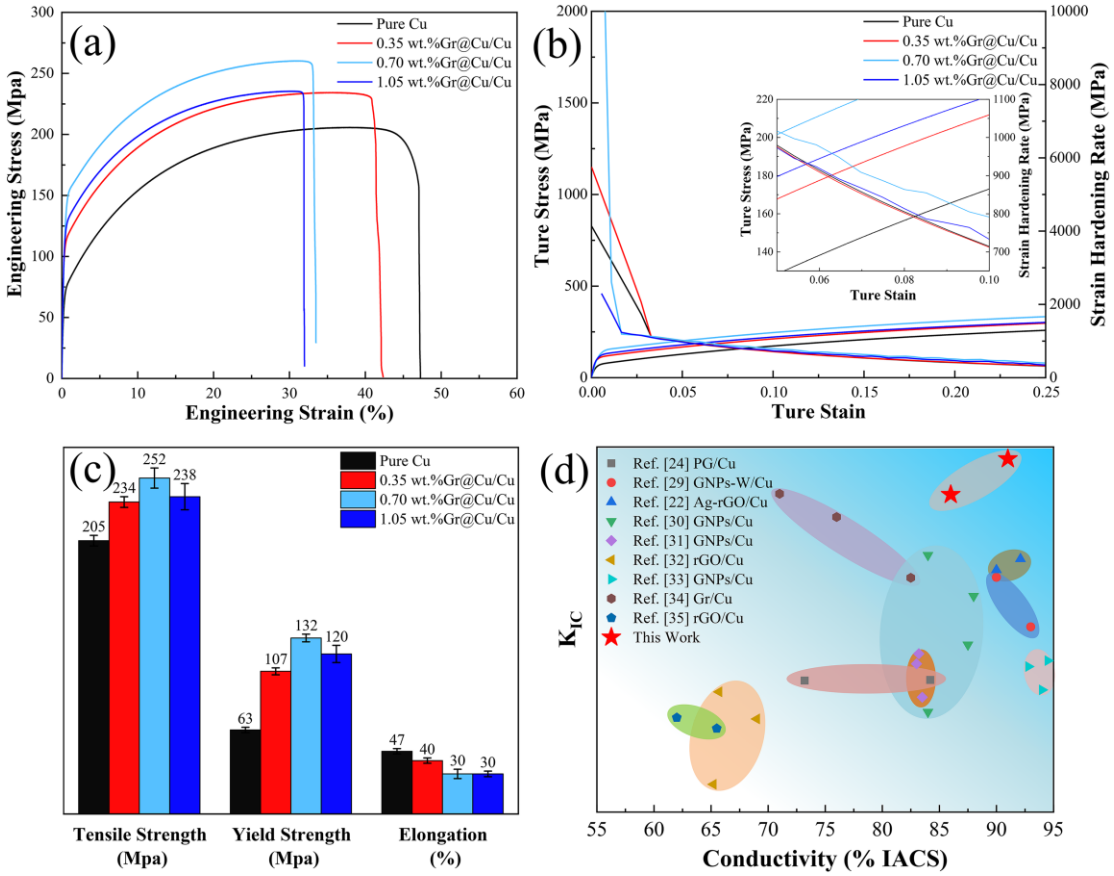

Fig. 8 Tensile properties of pure copper and Gr@Cu/Cu composites. (a) Engineering stress-strain curve, (b) real stress-strain curve, and real strain hardening rate curve, the inset is a partially enlarged view at the red dashed line. (c) numerical values and errors of ultimate tensile strength, yield strength, and elongation; (d) Comparisons of comprehensive performance of the Cu matrix composite with those reported in literature

The fracture morphologies of the sintered copper and composites are shown in Fig. 9. The tensile fracture surface of pure copper has a typical dimple morphology of typical plastic materials. A few holes (black arrows) can be seen in Fig. 9(a). Compared with that of pure copper, the fracture surfaces of Gr@Cu/Cu composites not only show plastic fracture characteristics (e.g., dimples), but also show brittle fracture characteristics (e.g., intergranular fracture). This mixed fracture mode links

well with the composite's good strength and ductility. The fracture surfaces of 0.35 wt.% and 0.70 wt.%Gr@Cu/Cu composites show partially broken Gr@Cu reinforced phases (red arrow in Figs. 9 (c) and (d)). This indicates that the interfacial bonding between graphene and the copper matrix was strong, and there was sufficient load transfer from the matrix to the reinforcement, which can break the graphene layer. Compared with the tensile fracture morphology of 0.35 wt.%Gr@Cu/Cu composite, the number of dimples in the fracture surfaces of 0.70 wt.%Gr@Cu/Cu composite is apparently reduced, and fracture of the reinforcement phase appears increased. Therefore, its strength has been increased and its plasticity has been decreased. When the graphene content reaches 1.05 wt.%, the graphene in the composites becomes agglomerated (outlined by the white dashed line in Fig. 9(e)), thus reducing the tensile properties and conductivity of the composite. In addition, the pull-out phenomena left by removing of the reinforcing phase can be found from the fracture morphology (see Figs. 9 (c), (d), and (e)), indicating that some of the graphenes are poorly bonded inside the copper matrix. This could be the key reason why in many studies of graphene reinforced copper matrix composites, the actual reinforcement value has not reached the expected reinforcement effect [12, 31, 36, 37].

The interfacial fracture processes between the graphene and the copper matrix may have the following stages. (1) The cracks are originated from the sintered holes or other defects, and then spread through the copper matrix to the surface of composites. When the graphene and the copper matrix are firmly bonded, the cracks are extended to the graphene layer through the interface, and then start to expand

laterally in the graphene until the Gr@Cu reinforcement phases are completely broken (e.g., the areas outlined by the yellow curve in Figs. 9 (f) and (g)). When the graphene is poorly bonded to the copper matrix, the cracks will propagate easily along the composite's interfaces, causing the quick separation of graphene and matrix. (2) Cracks are initiated from the interfacial defects and then propagate further outside.

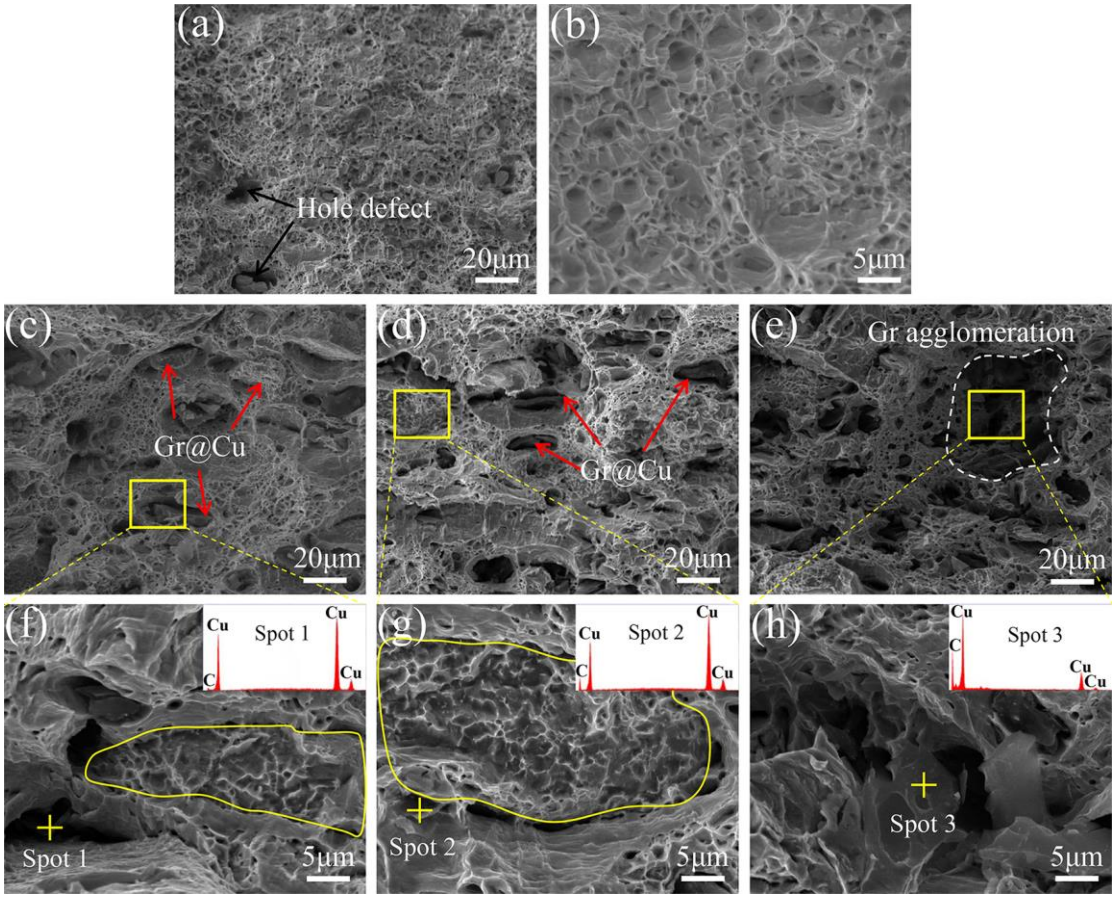

Fig. 9 SEM and EDS images of tensile fractures of pure copper and Gr@Cu/Cu composites. (a, b) Pure copper, (c, f) 0.35 wt.%Gr@Cu/Cu composite, (d, g) 0.70 wt.%Gr@Cu/Cu composite, (e, h) 1.05 wt.%Gr@Cu/Cu composite. The illustrations are the EDS images at A, B, and C

As we all know, the interfacial structures of the composite significantly affect the properties of composites. For example, some studies have pointed out that in the

rGO/Cu composites, oxygen-mediated phenomena (e.g., formation of Cu-O-Cu chemical bonds) occur at the interface, which will significantly improve the bonding of the composite's interface, thereby improving the comprehensive performance of the composite [38]. To prove if this is true for this study, the composite interface was characterized using TEM, and the obtained images are shown in Fig. 10. The interface is bonded well without obvious cracks (Fig. 10(a)). HRTEM image of the composite interface (Fig. 10(b)) reveals that a small amount of graphene exists at the interface, and there is no copper oxide at the interface. These results indicate that there is no oxygen-mediated interface at the interface of graphene and copper, which is consistent with the findings of Sun et al. [12] and Zhang et al. [38]. The smooth interface between graphene and copper generally follows the patterns of a two-dimensional morphology of graphene. Fast Fourier Transform (FFT) analysis shown in the inset of Fig. 10(b) reveals that the lattice orientation relationship is $Cu_{(111)}//Gr_{(002)}$. The lattice fringes of graphene are clearly bent and dislocations are generated, which are mainly caused by the large differences in thermal expansion coefficients between graphene and copper and their lattice spacings.

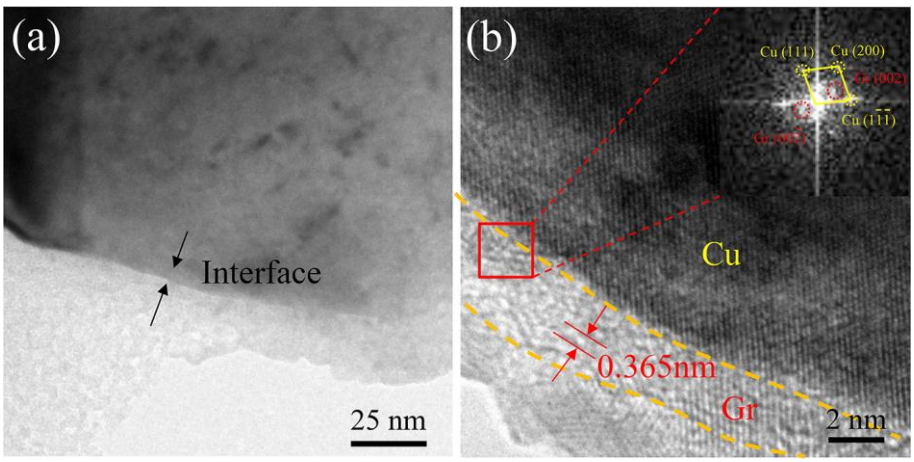

Fig. 10 TEM images of 0.70 wt.%Gr@Cu/Cu composites. (a) TEM, (b) HRTEM. The illustration is the FFT image of the red box in (b)

4. Conclusion

In this paper, wheat flour was applied as the solid precursor of graphene to *in-situ* generate graphene on the surface of copper powder. Wet mixing technology and SPS technology were used to add different contents of Gr@Cu composite powders into the copper matrix in order to obtain Gr@Cu/Cu composites.

(1) Applications of *in-situ* generation technology and wet mixing technology reduce the agglomeration of graphene in the copper matrix, and promote the formation of well-bonded interfacial structures. This enhances the load transfer capability of the composites.

(2) The density of the composite material obtained after the SPS sintering reaches 99%, which effectively delays the crack propagation and prevents the strong electron scattering effect.

(3) The fracture morphology of the sintered composite shows a mixed fracture mode, in which the pure copper matrix shows a typical plastic fracture, and the graphene shows an intergranular fracture.

(4) The interface between the graphene and the copper matrix is well bonded, with a lattice orientation relationship of $Cu_{(111)}//Gr_{(002)}$.

Acknowledgments

The authors would like to acknowledge the financial supports from Shaanxi Coal Industry Group United Fund of China (No.2019JLM-2), Xi'an Science research

project of China (No.2020KJRC0089) and Electrical Materials and Infiltration Key Laboratory of Shaanxi Province Projects (No.17JS080), and International Exchange Grant (IEC/NSFC/201078) through Royal Society and National Science Foundation of China (NSFC).

References

[1] H.R. Lin, H.F. Shao, Z.J. Zhang, H.J. Yang, J.C. Sun, L.B. Zhang, Z.F. Zhang, Stress relaxation behaviors and mechanical properties of precipitation strengthening copper alloys, J. Alloys Compd. 861 (2021) 158537.

[2] D.-P. Lu, J. Wang, W.-J. Zeng, Y. Liu, L. Lu, B.-D. Sun, Study on high-strength and high-conductivity Cu–Fe–P alloys, Mater. Sci. Eng.: A 421(1) (2006) 254-259.

[3] M. Gholami, J. Vesely, I. Altenberger, H.A. Kuhn, M. Janecek, M. Wollmann, L. Wagner, Effects of microstructure on mechanical properties of CuNiSi alloys, J. Alloys Compd. 696 (2017) 201-212.

[4] F. Yan, W. Chen, P. Feng, L. Dong, T. Yang, S. Ren, Y. Fu, Microstructure evolution and enhanced properties of Cu-Cr-Zr alloys through synergistic effects of alloying, heat treatment and low-energy cyclic impact, J. Mater. Res. 35(20) (2020) 2746-2755.

[5] R. Casati, M. Vedani, Metal Matrix Composites Reinforced by Nano-Particles-A Review, Metals 4(1) (2014) 65-83.

[6] W. Chen, T. Yang, L. Dong, A. Elmasry, J. Song, N. Deng, A. Elmarakbi, T. Liu, H.B. Lv, Y.Q. Fu, Advances in graphene reinforced metal matrix

nanocomposites: Mechanisms, processing, modelling, properties and applications, Nanotechnology and Precision Engineering 3(4) (2020) 189-210.

[7] A. Kozbial, Z. Li, C. Conaway, R. McGinley, S. Dhingra, V. Vahdat, F. Zhou, B. D'Urso, H. Liu, L. Li, Study on the Surface Energy of Graphene by Contact Angle Measurements, Langmuir 30(28) (2014) 8598-8606.

[8] F. Nazeer, Z. Ma, L. Gao, F. Wang, M.A. Khan, A. Malik, Thermal and mechanical properties of copper-graphite and copper-reduced graphene oxide composites, Composites Part B: Engineering 163 (2019) 77-85.

[9] S.C. Yoo, J. Lee, S.H. Hong, Synergistic outstanding strengthening behavior of graphene/copper nanocomposites, Composites Part B: Engineering 176 (2019) 107235.

[10] M. Cao, D.-B. Xiong, Z. Tan, G. Ji, B. Amin-Ahmadi, Q. Guo, G. Fan, C. Guo, Z. Li, D. Zhang, Aligning graphene in bulk copper: Nacre-inspired nanolaminated architecture coupled with in-situ processing for enhanced mechanical properties and high electrical conductivity, Carbon 117 (2017) 65-74.

[11] Z. Dong, Y. Peng, X. Zhang, D.-B. Xiong, Plasma assisted milling treatment for improving mechanical and electrical properties of in-situ grown graphene/copper composites, Composites Communications 24 (2021) 100619.

[12] C. Sun, X. Zhang, N. Zhao, C. He, Influence of spark plasma sintering temperature on the microstructure and strengthening mechanisms of

discontinuous three-dimensional graphene-like network reinforced Cu matrix composites, Mater. Sci. Eng.: A 756 (2019) 82-91.

[13] Z. Yang, L. Wang, Y. Cui, Z. Shi, M. Wang, W. Fei, High strength and ductility of graphene-like carbon nanosheet/copper composites fabricated directly from commercial oleic acid coated copper powders, Nanoscale 10(36) (2018) 16990-16995.

[14] M. Wang, J. Sheng, L.-D. Wang, Z.-Y. Yang, Z.-D. Shi, X.-J. Wang, W.-D. Fei, Hot rolling behavior of graphene/Cu composites, J. Alloys Compd. 816 (2020) 153204.

[15] H. Yue, L. Yao, X. Gao, S. Zhang, E. Guo, H. Zhang, X. Lin, B. Wang, Effect of ball-milling and graphene contents on the mechanical properties and fracture mechanisms of graphene nanosheets reinforced copper matrix composites, J. Alloys Compd. 691 (2017) 755-762.

[16] J. Hwang, T. Yoon, S.H. Jin, J. Lee, T.-S. Kim, S.H. Hong, S. Jeon, Enhanced Mechanical Properties of Graphene/Copper Nanocomposites Using a Molecular-Level Mixing Process, Adv. Mater. 25(46) (2013) 6724-6729.

[17] S. Shu, Q. Yuan, W. Dai, M. Wu, D. Dai, K. Yang, B. Wang, C.-T. Lin, T. Wuebben, J. Degenhardt, C. Regula, R. Wilken, N. Jiang, J. Ihde, In-situ synthesis of graphene-like carbon encapsulated copper particles for reinforcing copper matrix composites, Mater. Design 203 (2021) 109586.

[18] K. Chu, C. Jia, Enhanced strength in bulk graphene–copper composites, Physica Status Solidi 211(1) (2014) 184-190.

[19] K. Rajkumar, S. Aravindan, Tribological behavior of microwave processed copper–nanographite composites, Tribology International 57 (2013) 282-296.

[20] C. Salvo, R.V. Mangalaraja, R. Udayabashkar, M. Lopez, C. Aguilar, Enhanced mechanical and electrical properties of novel graphene reinforced copper matrix composites, J. Alloys Compd. 777 (2019) 309-316.

[21] C. Ayyappadas, A. Muthuchamy, A. Raja Annamalai, D.K. Agrawal, An investigation on the effect of sintering mode on various properties of copper-graphene metal matrix composite, Advanced Powder Technology 28(7) (2017) 1760-1768.

[22] T. Yang, W. Chen, F. Yan, H. Lv, Y.Q. Fu, Effect of reduced graphene oxides decorated by Ag and Ce on mechanical properties and electrical conductivity of copper matrix composites, Vacuum 183 (2021) 109861.

[23] S.Y. Qian, Z.H. Xu, H.N. Xie, C.S. Shi, N.Q. Zhao, C.N. He, E.Z. Liu, Effect of rare metal element interfacial modulation in graphene/Cu composite with high strength, high ductility and good electrical conductivity, Appl. Surf. Sci. 533 (2020) 147489.

[24] R. Jiang, X. Zhou, Q. Fang, Z. Liu, Copper–graphene bulk composites with homogeneous graphene dispersion and enhanced mechanical properties, Materials Science and Engineering A 654 (2016) 124-130.

[25] W.M. Daoush, B.K. Lim, C.B. Mo, D.H. Nam, S.H. Hong, Electrical and mechanical properties of carbon nanotube reinforced copper nanocomposites

fabricated by electroless deposition process, Mater. Sci. Eng.: A 513-514 (2009) 247-253.

[26] S. Nachum, N.A. Fleck, M.F. Ashby, A. Colella, P. Matteazzi, The microstructural basis for the mechanical properties and electrical resistivity of nanocrystalline Cu–Al2O3, Mater. Sci. Eng.: A 527(20) (2010) 5065-5071.

[27] K. Chu, F. Wang, Y.-b. Li, X.-h. Wang, D.-j. Huang, Z.-r. Geng, Interface and mechanical/thermal properties of graphene/copper composite with Mo2C nanoparticles grown on graphene, Compos. Part A: App. S. 109 (2018) 267-279.

[28] X. Zheng, On an unified model for predicting notch strength and fracture toughness of metals, Engineering Fracture Mechanics 33(5) (1989) 685-695.

[29] L.L. Dong, Y.Q. Fu, Y. Liu, J.W. Lu, W. Zhang, W.T. Huo, L.H. Jin, Y.S. Zhang, Interface engineering of graphene/copper matrix composites decorated with tungsten carbide for enhanced physico-mechanical properties, Carbon 173 (2021) 41-53.

[30] F. Chen, J. Ying, Y. Wang, S. Du, Z. Liu, Q. Huang, Effects of graphene content on the microstructure and properties of copper matrix composites, Carbon 96 (2016) 836-842.

[31] X. Si, M. Li, F. Chen, P. Eklund, J. Xue, F. Huang, S. Du, Q. Huang, Effect of carbide interlayers on the microstructure and properties of graphene-nanoplatelet-reinforced copper matrix composites, Mater. Sci. Eng.: A 708 (2017) 311-318.

[32] Z. Yang, L. Wang, Z. Shi, M. Wang, Y. Cui, B. Wei, S. Xu, Y. Zhu, W. Fei, Preparation mechanism of hierarchical layered structure of graphene/copper composite with ultrahigh tensile strength, Carbon 127 (2018) 329-339.

[33] M. Yang, L. Weng, H. Zhu, T. Fan, D. Zhang, Simultaneously enhancing the strength, ductility and conductivity of copper matrix composites with graphene nanoribbons, Carbon 118 (2017) 250-260.

[34] F. Chen, Q.S. Mei, J.Y. Li, C.L. Li, L. Wan, G.D. Zhang, X.M. Mei, Z.H. Chen, T. Xu, Y.C. Wang, Fabrication of graphene/copper nanocomposites via in-situ delamination of graphite in copper by accumulative roll-compositing, Composites Part B: Engineering 216 (2021) 108850.

[35] L. Wang, Z. Yang, Y. Cui, B. Wei, S. Xu, J. Sheng, M. Wang, Y. Zhu, W. Fei, Graphene-copper composite with micro-layered grains and ultrahigh strength, Sci. Rep. 7(1) (2017) 41896.

[36] S. Guo, X. Zhang, C. Shi, E. Liu, C. He, F. He, N. Zhao, In situ synthesis of high content graphene nanoplatelets reinforced Cu matrix composites with enhanced thermal conductivity and tensile strength, Powder Technol. 362 (2020) 126-134.

[37] K. Zhang, G. Shao, X. Chen, W. Li, F. Ma, P. Liu, Study of mechanical properties of graphene nanoplates reinforced copper matrix composites prepared through electrostatic self-assembly and electroless copper plating, Mater. Lett. 252 (2019) 338-341.

[38] X. Zhang, C. Shi, E. Liu, N. Zhao, C. He, Effect of Interface Structure on the Mechanical Properties of Graphene Nanosheets Reinforced Copper Matrix Composites, ACS Appl. Mater. Inter. 10(43) (2018) 37586-37601.